

Phase transition to frequency entrainment in a long chain of pulse-coupled oscillators

Per Östborn*

Department of Mathematical Physics, Lund University, S-221 00 Lund, Sweden

(Received 31 May 2001; published 12 July 2002)

A long chain of pulse-coupled oscillators was studied. The oscillators interacted via a phase response curve similar to those obtained from pacemaker cells in the heart. The natural frequencies were random numbers from a distribution with finite bandwidth. Stable frequency-entrained states were shown always to exist above a critical coupling strength. Below the critical coupling, the probability to have such states was shown to be zero if the number of oscillators is infinite. This discontinuity establishes the existence of a phase transition in the thermodynamic limit. For weak coupling, clusters of frequency-entrained oscillators emerged. The cluster sizes were exponentially distributed, even when the critical coupling was approached. At this coupling, the mean cluster size diverged to infinity according to a power law. The standard deviation of the distribution of mean frequencies in the chain converged to zero, also according to a power law.

DOI: 10.1103/PhysRevE.66.016105

PACS number(s): 05.70.Fh, 05.45.Xt

I. INTRODUCTION

The idea to compare frequency entrainment in oscillator networks with phase transitions is natural and not new [1–3]. If the natural frequencies are not all the same, there is a degree of disorder, or “temperature,” which has to be overcome by mutual coupling if all oscillators are to “freeze” into the same frequency. There is a difference compared to ordinary phase transitions though. Entraining oscillator networks are dissipative nonequilibrium systems.

To be able to analyze the problem in the thermodynamic limit where the number N of oscillators goes to infinity, very simple models for the individual oscillators have to be used. The simplest choice is to describe the state of the oscillator by a single phase $\phi \in [0, 1)$. In such oscillator communities, Winfree [1] and Kuramoto [3] have shown, for two different kinds of smooth interaction, that there was a stable frequency-entrained state whenever the coupling exceeded a critical level. They assumed random natural frequencies and homogeneous global coupling.

More realistic networks have spatial structure, i.e., the coupling is local. Kuramoto [3] hypothesized that, in such systems with random frequencies one should find clusters of entrained oscillators [4], and that at a critical coupling level one cluster becomes macroscopic, i.e., $O(N)$ as $N \rightarrow \infty$. This would signal a phase transition. The clusters are defined to be connected sets of oscillators with identical mean frequency. In this paper, a phase transition of this kind is demonstrated analytically and studied numerically. To the best of my knowledge this has not been done before. Earlier work in this area has not revealed conclusive results. Sakaguchi, Shinomoto, and Kuramoto [5] searched for this kind of phase transition in the system

$$\dot{\phi}_k = 1/P_k + K \sum_{l \in n_k} \sin[2\pi(\phi_l - \phi_k)]. \quad (1)$$

P_k is the natural period of oscillator k , and n_k is the set of oscillators coupled to k . In their simulations, they found fre-

quency clusters which appeared to become macroscopic for a finite critical K , if the lattice dimension $d > 2$. However, Strogatz and Mirollo [6] showed later that, in the thermodynamic limit, for any d and for any finite K , the probability of having frequency entrainment in system (1) was zero for any random distribution of P_k with nonzero bandwidth. However, the possibility of seeing sponge-like macroscopic clusters could not be excluded. Therefore it is still an open question whether a critical K exists for $d > 2$. The proof of Mirollo and Strogatz rested on the fact that the sine function is odd. For a slightly different kind of interaction, Sakaguchi, Shinomoto, and Kuramoto [7] gave a heuristic argument why an arbitrarily long chain of oscillators with a limited frequency bandwidth may frequency entrain. Kopell and Ermentrout [8] also pointed out that a nonodd interaction enables entrainment in an arbitrarily long chain with a linear frequency gradient with fixed frequency difference between the ends. Later, they showed that frequency entrainment can be present even if the frequencies do not change monotonically in the chain [30]. However, they assumed that $|P_{k+1} - P_k| = O(1/N)$. This smoothness condition does not allow random frequencies. Rogers and Wille [9] studied system (1) in the form of a chain with “quasi-local” interaction. The coupling strength was proportional to $r^{-\alpha}$, where r is the distance between the interacting oscillators. They found numerically that entrainment emerged in the thermodynamic limit below a critical value of α .

Another class of interaction is pulse coupling. In such models, an oscillator affects its neighbors only when its phase is one. This type of model is often adequate to describe assemblies of biological oscillators. For example, muscle cells and neurons perturb their neighbors primarily when they fire action potentials. These are well defined in time. Inspired by this fact, one says that a pulse-coupled oscillator “fires” when $\phi = 1$.

Ikeda [10] and Brailove [11] have analyzed the dynamics of a pair of pulse-coupled oscillators with different natural frequencies. To my knowledge, the behavior of larger pulse-coupled oscillator networks has not previously been analyzed in the case where the oscillators are locally coupled and non-identical. Mirollo and Strogatz [12] showed that certain kinds of globally coupled, identical oscillators almost always

*Electronic address: per.ostborn@matfys.lth.se

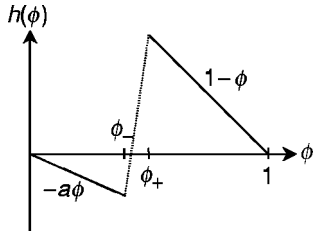


FIG. 1. The term $gh(\phi)$ is the phase response curve (PRC) used in system (2). From the requirement $0 \leq \phi + gh(\phi) < 1$, we have $g < 1$ and $a \leq 1$. In the analysis, $h(\phi)$ is left undefined in the region $\phi_- < \phi < \phi_+$, where $0 < \phi_- < \phi_+ < 1$. In the simulations, the straight dotted line connected $h(\phi_-)$ with $h(\phi_+)$, where $\phi_- = 0.4$ and $\phi_+ = 0.5$. The resulting PRC is reasonable to model interactions between sinus node cells in the weak coupling regime.

synchronize. Locally coupled, identical oscillators have also been analyzed [13]. Recently, conditions for synchronization of globally coupled nonidentical oscillators were also given [14]. The word synchronization is used here to denote a state where all oscillators fire at the same time, at a constant frequency. In a frequency-entrained state, time lags between firings may exist.

In this paper, a pulse-coupled oscillator network of the form

$$\dot{\phi}_k = 1/P_k + gh(\phi_k) \sum_{l \in n_k} \delta(\phi_l) \quad (2)$$

is studied. The term $gh(\phi_k)$ is the phase response curve (PRC), where g is the coupling strength. In words, the dynamics of the system is as follows: $\dot{\phi}_k = 1/P_k$ when no neighbor $l \in n_k$ fires. When one neighbor does fire, ϕ_k immediately jumps by the amount $gh(\phi_k)$. The PRC used here is inspired by experiments on sinus node cells [15], and has the form described in Fig. 1. P_k was taken from a random distribution with finite bandwidth. A one-dimensional chain with bidirectional nearest-neighbor coupling was used. This made it possible to establish analytically the existence of a finite critical coupling g_c .

The sinus node is the natural pacemaker of the heart, and consists of more than 100 000 cells [16]. In most of these, action potentials are generated at a given natural frequency, which differs from cell to cell [17]. Despite this, the entire node normally entrains to a common frequency, thus initiating regular heartbeats. This is achieved for an electric coupling much weaker than in the rest of the heart [18]. This fact indicates that a phase transition of the Kuramoto kind may arise in oscillator networks similar to the sinus node, such as system (2) with the PRC in Fig. 1. Loss of frequency entrainment in the sinus node might be one substrate behind some cardiac arrhythmias [19].

Peskin [20] proposed another type of model for cardiac pacemaker cells. This type is often used in analytical studies of pulse-coupled oscillator networks [11–14]. However, at least in the case of cardiac pacemakers, it is not very realistic. First, only positive phase shifts are allowed, contrary to experimental evidence [15]. Second, if the phase of an oscillator receiving a pulse is large enough, its phase is immedi-

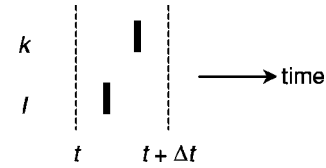


FIG. 2. Illustration of how the possible error in the inexact integration method arises. The bars represent firings of the oscillators k and l .

ately brought to one. This means that the velocity of firing waves propagating through the network can be infinite. This is unphysiological and even unphysical. It seems that there should be time lags between the firings of the oscillators in every realistic, frequency-entrained model network of non-identical oscillators. In the rabbit sinus node, the time lag of the periphery compared to the center is roughly 10% of the firing period [21]. Sometimes, strict synchrony seems to be a good approximation, e.g., in swarms of fireflies flashing with the same frequency. However, waves of light through the swarms have also been reported [22].

The PRC gh in Fig. 1 belongs to a family of PRCs u for which $u(0) = 0$ and u is bipolar, with $u < 0$ for small phases, and $u > 0$ for large phases. The PRC in Fig. 1 may be seen as a linearization of such a general PRC around $\phi = 0$. Apart from sinus node cells, PRCs of many other biological oscillators belong to this family. For example, the calling cycle of crickets is perturbed in this way when they hear a call [2]. Such a PRC also applies to the flashing cycle of the firefly species *pteroptyx malaccae* when affected by flashes [22], slime mold cells as they react to cAMP [2], and segments of the lamprey spinal cord responding to electrical impulses [23]. Therefore, the analysis of system (2) with this kind of PRC is of general interest.

II. NUMERICAL METHODS

There are exact ways to integrate system (2) numerically. Unfortunately the computation time is $\propto N^2$, making them unsuitable for this study. Instead an inexact method was used, with computation time $\propto N$.

One inexact method is to use a constant time step Δt which is small compared to the natural periods. Given the vector of phases $\phi(t)$, preliminary new phases for each oscillator are calculated according to $\tilde{\phi}_k(t + \Delta t) = \phi_k(t) + \Delta t/P_k$. Then, in a predefined order, it is checked whether $\tilde{\phi}_k(t + \Delta t) \geq 1$ for each k . In that case $\tilde{\phi}_k(t + \Delta t) \rightarrow \tilde{\phi}_k(t + \Delta t) - 1$, and a firing of k is registered at time $t'_k = t + \Delta t - \tilde{\phi}_k(t + \Delta t)P_k$. If $l \in n_k$, then $\tilde{\phi}_l(t + \Delta t) \rightarrow \tilde{\phi}_l(t + \Delta t) + gh[(\phi_l(t) + (t'_k - t)/P_l)]$. When all oscillators are checked, $\phi(t + \Delta t) = \tilde{\phi}(t + \Delta t)$ is assigned.

This method is inexact if and only if the following situation appears (Fig. 2). Suppose that, in the exact solution, k fires in the time interval $(t, t + \Delta t)$ and that $l \in n_k$ also does so, but before k . Suppose also that the checking order is such that k is handled before l . Then the firing instant t'_k of k is

determined without taking into account the phase jump it receives from l . The incorrect t'_k means that the phase jump l receives from k becomes incorrect, and consequently, when l is subsequently handled, its firing instant will be slightly wrong. This in turn means that the phase jump k receives from l will be erroneous. Evidently, the probability that this occurs decreases with Δt , i.e., the accuracy increases when Δt is made smaller.

The algorithm can be modified to make it exact. Then, in the same way as before, firing instants \tilde{t}'_k are calculated for all oscillators whose preliminary phase has exceeded one during the time step. This time the firing instants are only preliminary. The number $t'_m = \min\{\tilde{t}'_k\}$ is registered as the actual firing instant of oscillator m , its phase is reduced by one, and pulses are delivered to its neighbors as before. Then new preliminary firing instants are calculated for the oscillators whose phases still exceed one. The process is repeated until no oscillator has $\tilde{\phi}_k(t + \Delta t) \geq 1$. Then $\phi(t + \Delta t) = \tilde{\phi}(t + \Delta t)$.

The difference is that in the exact method, the oscillator that fires first is handled first, whereas the handling order is predefined in the inexact method. The computation time becomes $\propto N^2$ since to register the firing of one oscillator, $\mathcal{O}(N)$ preliminary firing instants \tilde{t}'_k have to be checked to find the smallest one. Note that the choice of Δt is irrelevant as long as the same oscillator never fires twice in a time step.

In this study a compromise between the two methods was used. The chain was divided into groups of m oscillators. Within each group, the oscillator that fired first was handled first. Therefore the situation in Fig. 2 never appeared *within* a group. It could only appear at a group border. Evidently, the accuracy of this method increases with m , becoming exact for $m = N$.

For $1 \leq P_k \leq 1.5$, I chose $\Delta t = 0.01$ and $m = 25$ after comparing accuracy and computation times for different parameter values. The raw material for the numerical analysis in this study is the mean periods of the individual oscillators. To compute these, assuming that they exist, the system should have reached its attractor, after which they should be measured during an infinitely long time. Of course, a finite transient time T_t and a finite measurement time T_m had to be chosen. The data presented are computed for $T_t = T_m = 1000$. For chains of 100 oscillators, the error in the mean periods computed in this way was typically < 0.001 , where the exact integration method with $T_t = T_m = 50\,000$ was used as reference. In all simulations the initial condition $\phi = 0$ was used.

The finite integration time means that frequency clusters are not perfectly defined. Two neighbor oscillators were said to belong to the same cluster if and only if the mean period difference was less than $\delta P = 0.002$. Note that the difficulty in discriminating clusters does not arise, for example, in lattices of discrete spins, such as the Ising model.

III. EXISTENCE OF A PHASE TRANSITION

In this section the existence of a finite critical coupling is proved. This guarantees that the apparent phase transition

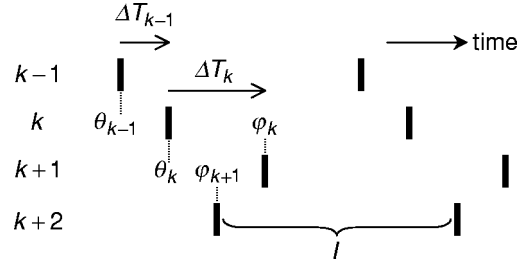


FIG. 3. Parameters describing an entrained state. Bars represent firing instants ($\phi = 1$). The term φ_k is the phase in the cycle of oscillator k just before $k+1$ fires. θ_k is the phase in the oscillator $k+1$ cycle just before k fires. The requirements expressed in Eq. (4) make it possible to associate a given firing of k with one of $k+1$. ΔT_k is the time (with sign) from the firing of k to the associated firing of $k+1$.

seen in the simulations (Sec. IV) is not a numerical artifact. We focus on a certain kind of entrained states, and prove some properties of these. Loosely speaking, proposition 1 states that such states always exist if $g > g_c$. Proposition 2 states that for $g < g_c$, the probability is zero to have such states in the thermodynamic limit. This discontinuity in the probability establishes the existence of a phase transition. Proposition 3 states that the states are stable, so that they can actually be observed. Proposition 2 also states that in the thermodynamic limit, the entrained frequency is almost always that of the fastest oscillator. In contrast, for system (1) the entrained frequency is always the mean of the natural frequencies [6].

A system of type (2) is assumed, with h given by Fig. 1. The oscillators are coupled bidirectionally with their nearest neighbors in a chain with open ends. If $g = 1$, the coupling can be said to be infinite. Then, if oscillator k fires when $\phi_{k+1} \geq \phi_+$, $\phi_{k+1} \rightarrow \phi_{k+1} + h(\phi_{k+1}) = \phi_{k+1} + (1 - \phi_{k+1}) = 1$, so that oscillator $k+1$ will immediately fire. The firing transmission velocity is infinite. In this case, it is not hard to see that there is an entrained state in which all oscillators fire synchronously if and only if $P_{\min}/P_{\max} \geq \phi_+$. Generally, an entrained state can be described as in Fig. 3. It is specified by the entrained period I , and one of the vectors θ or φ , which both have length $N-1$. We have

$$P_k = I + gh(\theta_{k-1})P_k + gh(\varphi_k)P_k. \quad (3)$$

(The θ_{k-1} and φ_k terms vanish for $k=1$ and N , respectively.) We focus on entrained states for which

$$\theta_k, \varphi_k \in [0, \phi_-) \quad \text{or} \quad (\phi_+, 1), \quad (4)$$

$$\theta_k \in [0, \phi_-) \Leftrightarrow \varphi_k \in (\phi_+, 1),$$

for all k . The second condition means that two neighbor oscillators are not allowed to trigger each other, or delay each other. This implies that a given firing of k can be associated unambiguously with one firing of $k+1$. The time difference ΔT_k between the associated firings is defined to be positive if and only if the firing of k occurs first, where the firing of k is said to occur first if and only if $\theta_k \in (\phi_+, 1)$. We have $\theta_{k-1} = \theta_{k-1}(P_k, \Delta T_{k-1}, \Delta T_k)$ and $\varphi_k = \varphi_k(P_k,$

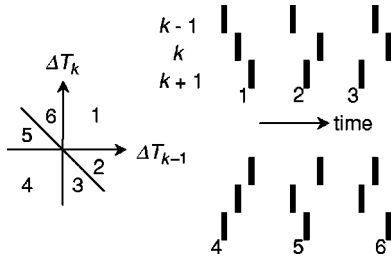


FIG. 4. The function $P_k = f_k(I, \Delta T_{k-1}, \Delta T_k)$ [Eq.(5)] is piecewise linear. It is linear in each of the six regions marked. The firing order in each case is shown (cf. Fig. 3).

$\Delta T_{k-1}, \Delta T_k$). Using the sign function $s(x) = 1$ for $x \geq 0$ and $s(x) = -1$ for $x < 0$, and letting $b(x) = a$ for $x \geq 0$ and $b(x) = 1$ for $x < 0$, it can be checked that

$$P_k = I + gb(-\Delta T_{k-1})[1 - b(-\Delta T_{k-1})g]^{q_k} \Delta T_{k-1} - gb(\Delta T_k)[1 - b(\Delta T_k)g]^{r_k} \Delta T_k, \quad (5)$$

where

$$q_k = s(\Delta T_{k-1} + \Delta T_k)/2 - s(\Delta T_{k-1}) - 1/2,$$

$$r_k = -s(\Delta T_{k-1} + \Delta T_k)/2 + s(\Delta T_k) - 1/2.$$

(The ΔT_{k-1} and ΔT_k terms vanish for $k = 1$ and N , respectively.) Equation (5) expresses a continuous, piecewise linear, and invertible function $P = f(I, \Delta T)$. We get six different linear cases, depending on the relation between ΔT_{k-1} and ΔT_k (Fig. 4). For example, in case 1 we have

$$P_k = I + g(1-g)^{-1} \Delta T_{k-1} - ag \Delta T_k. \quad (5')$$

It is not hard to see that Eq. (5') follows from Eq. (3) since in this case $P_k = I + g(1 - \theta_{k-1})P_k + ag \varphi_k P_k$, and referring to Fig. 3, $\Delta T_{k-1} = (1-g)(1 - \theta_{k-1})P_k$ and $\Delta T_k = \varphi_k P_k$.

Proposition 1. Let $P_{\min} \leq P_k \leq P_{\max}$. Then there exists an entrained state fulfilling Eq. (4) whenever $g > g_c$, where g_c is given by

$$(1-g_c)g_c^{-1}(1+ag_c-a)^{-1}(P_{\max}-P_{\min}) = \min\{\phi_- P_{\min}, (1-g_c)(1-\phi_+)P_{\max}\}. \quad (6)$$

The requirement $g_c \leq 1$ sets the limit $P_{\min}/P_{\max} \geq \phi_+$. Within this limit we seek the set of P for which $(I, \Delta T) = f^{-1}(P)$ at a given g is an entrained state which fulfills Eq. (4). However, f seems practically impossible to invert in general. To prove Proposition 1, we instead make use of the following two lemmas. The idea of the proof is expressed in Fig. 5.

Lemma 1. Let $P = (P_1, \dots, P_N)$ with $P_{\min} \leq P_k \leq P_{\max}$. If and only if $g > g_c$, it is possible for any such P to construct an entrained state $(P_{\min}, \Delta T')$ fulfilling Eq. (4) with $\Delta T'_k \geq 0, \forall k$ for $P' = (P'_1, P_2, \dots, P_N)$, where $P'_1 \leq P_{\min}$. Under the same conditions it is possible to construct a state $(P_{\min}, \Delta T'')$ with $\Delta T''_k \leq 0, \forall k$ for $P'' = (P_1, \dots, P_{N-1}, P''_N)$, where $P''_N \leq P_{\min}$.

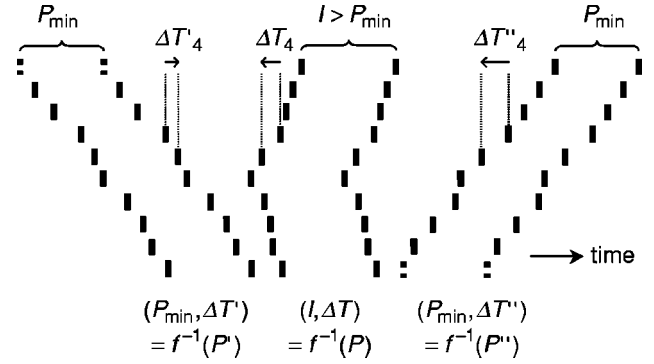


FIG. 5. Illustration of how proposition 1 is proved. The entrained states $f^{-1}(P')$ and $f^{-1}(P'')$ are constructed as described in the proof of Lemma 1. By increasing the period of the first oscillator from P'_1 to P_1 , we get the state $f^{-1}(P)$ from $f^{-1}(P')$. By then decreasing the period of oscillator N from P_N to P''_N , the state $f^{-1}(P'')$ is reached. In both processes all $\Delta T'_k$ decreases, so that $\Delta T'_k \geq \Delta T_k \geq \Delta T''_k$. This bound means that $f^{-1}(P)$ is a proper entrained state whenever $f^{-1}(P')$ and $f^{-1}(P'')$ are. In the figure, the vector $P = (1.37, 1.21, 1.22, 1.50, 1.23, 1.00, 1.42, 1.26, 1.10, 1.34)$ was used for $g = 0.65$ and $a = 1$ (Fig. 1).

Proof of Lemma 1. Locate a bar representing a firing instant of oscillator N (Fig. 5). Locate the associated bar of $N-1$ to the left of N so that N receives a positive phase jump such that its firing interval becomes P_{\min} . Locate the bar of $N-2$ to the left of $N-1$, so that $N-1$ also entrains to P_{\min} . This is repeated until the bar of oscillator 1 is placed to the left of 2, so that 2 fires with interval P_{\min} . This will happen at some $\Delta T'_1 = \Delta T'_1(P_{\min}, P_2, \dots, P_N) \geq 0$. If oscillator 1 is to entrain to P_{\min} , its natural period must be $P'_1 = P_{\min} - ag \Delta T'_1$.

Since they shall entrain to P_{\min} , no oscillator shall be delayed. Therefore $\Delta T'_{k-1} \geq 0$ if $\Delta T'_k \geq 0$. Also, $\Delta T'_{N-1} \geq 0$, so that $\Delta T'_k \geq 0, \forall k$. Thus the procedure can fail only if $\Delta T'_k$ at some stage in the construction becomes so large that Eq. (4) no longer holds. The worst situation in this respect is when a long section of the chain where all oscillators have natural period P_{\max} is to be entrained to P_{\min} . If j belongs to this section, it follows from Eq. (5') that for $a > 0$, $\Delta T'_j < \Delta T_{\max} \Leftrightarrow \Delta T'_j < \Delta T'_{j-1} < \Delta T_{\max}$ with $\Delta T_{\max} = (1-g)g^{-1}(1+ag-a)^{-1}(P_{\max}-P_{\min})$. For an infinitely long section of this kind, the $\Delta T'_k$'s will grow monotonically as k decreases, and saturate at the limit ΔT_{\max} [24]. Say that the section ends at oscillator k , i.e., $P_k = P_{\max}$, but $P_{k-1} < P_{\max}$. We have $\Delta T'_{k-1} = \Delta T_{\max}$. Equation (4) then requires $\Delta T_{\max} \leq \min\{\phi_- P_{k-1}, (1-g)(1-\phi_+)P_{\max}\}$. This condition is most restrictive if $P_{k-1} = P_{\min}$. Therefore, Eq. (7) follows. In the case $a = 0$, given that $P_k = P_{\max}$, $\Delta T'_{k-1} = \Delta T_{\max}$ regardless of the other natural periods.

The state $(P_{\min}, \Delta T'')$ is constructed in the same way, starting with oscillator 1 instead of N . Of course we get the same g_c . ■

Lemma 2. If $a > 0$, $\partial \Delta T_k / \partial P_1 < 0, \forall k$, and $\partial \Delta T_k / \partial P_N > 0, \forall k$. Also, $\partial I / \partial P_1 > 0$ and $\partial I / \partial P_N > 0$.

Proof of Lemma 2. Equation (5) has the form

$$P_k = I + c_{k1}\Delta T_{k-1} - c_{k2}\Delta T_k, c_{kj} > 0$$

for all ΔT if $a > 0$. We may write

$$\begin{aligned} \partial\Delta T_1/\partial P_1 &= c_{12}^{-1}\partial I/\partial P_1 - c_{12}^{-1} \\ &\vdots \\ \partial\Delta T_k/\partial P_1 &= c_{k2}^{-1}\partial I/\partial P_1 \\ &\quad + c_{k1}c_{k2}^{-1}\partial\Delta T_{k-1}/\partial P_1 \\ &\vdots \\ \partial\Delta T_{N-1}/\partial P_1 &= c_{N-1,2}^{-1}\partial I/\partial P_1 \\ &\quad + c_{N-1,1}c_{N-1,2}^{-1}\partial\Delta T_{N-2}/\partial P_1 \\ \partial\Delta T_{N-1}/\partial P_1 &= -c_{N1}^{-1}\partial I/\partial P_1. \end{aligned} \quad (7)$$

Assume that $\partial I/\partial P_1 \leq 0$. Then $\partial\Delta T_1/\partial P_1 < 0$ from the first row of Eq. (7), $\partial\Delta T_2/\partial P_1 < 0$ from the second, and so on. From the next to last row we get $\partial\Delta T_{N-1}/\partial P_1 < 0$, while we get $\partial\Delta T_{N-1}/\partial P_1 \geq 0$ from the last row. We have a contradiction. Thus $\partial I/\partial P_1 > 0$. Therefore, $\partial\Delta T_{N-1}/\partial P_1 < 0$ from the last row, $\partial\Delta T_{N-2}/\partial P_1 < 0$ from the next to last, and so on, so that $\partial\Delta T_k/\partial P_1 < 0, \forall k$. That $\partial I/\partial P_N > 0$ and $\partial\Delta T_k/\partial P_N > 0, \forall k$, can be shown analogously, or seen by symmetry. ■

Proof of Proposition 1. Suppose that $g > g_c$. Then the entrained states $(P_{\min}, \Delta T') = f^{-1}(P')$ and $(P_{\min}, \Delta T'') = f^{-1}(P'')$ exist according to Lemma 1. By increasing the period of oscillator 1 continuously from P'_1 to P_1 , leaving all other periods unchanged, the solution $(P_{\min}, \Delta T) = f^{-1}(P)$ is reached. $\partial\Delta T_k/\partial P_1 < 0, \forall k$ according to Lemma 2, giving $\Delta T'_k \geq \Delta T_k, \forall k$. By decreasing the period of oscillator N from P_N to P'_N , the state $f^{-1}(P'')$ is reached from $f^{-1}(P)$. $\partial\Delta T_k/\partial P_N > 0, \forall k$ according to Lemma 2, giving $\Delta T'_k \geq \Delta T_k \geq \Delta T''_k, \forall k$. Since $\partial I/\partial P_{1,N} > 0$ (Lemma 2), we also have $I \geq P_{\min}$. In summary

$$\begin{aligned} \Delta T'_k &\geq \Delta T_k \geq \Delta T''_k, \\ I &\geq P_{\min}. \end{aligned} \quad (8)$$

The three solutions $f^{-1}(P')$, $f^{-1}(P)$, and $f^{-1}(P'')$ are shown in Fig. 5 for a chain of ten oscillators. It may seem evident from Eq. (8) that $f^{-1}(P)$ is an entrained state fulfilling Eq. (4) whenever $f^{-1}(P')$ and $f^{-1}(P'')$ are, but we prove it below to make the treatment complete.

Around k , the state $f^{-1}(P)$ may belong to any of the six classes in Fig. 4. (The end-point oscillators 1 and N may be treated in the same setting by introducing $\Delta T_0 = 0$ and $\Delta T_N = 0$.) Let θ' and φ' be the phase vectors (Fig. 3) belonging to the state $f^{-1}(P')$, θ and φ those belonging to the solution $f^{-1}(P)$, and θ'' and φ'' the ones belonging to state $f^{-1}(P'')$. For notational simplicity, we re-express the first part of condition (4) as $\phi_+ - 1 < \varphi_k, \theta_k < \phi_-$, i.e., we let the phases vary in a continuous, partly negative interval. If we show that

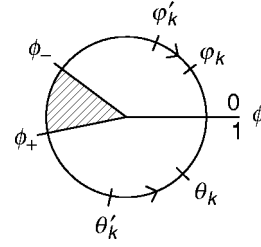


FIG. 6. Illustration of why the phases θ_k, φ_k belonging to the state $f^{-1}(P)$ fulfill the second part of Eq. (4) when θ'_k, φ'_k belonging to $f^{-1}(P')$ do so. See proof of Proposition 1 for explanation.

$$\begin{aligned} \theta'_{k-1} &\leq \theta_{k-1} \leq \theta''_{k-1}, \\ \varphi'_k &\geq \varphi_k \geq \varphi''_k, \end{aligned} \quad (9)$$

in this notation, then the solution $f^{-1}(P)$ fulfills the first part of Eq. (4), since θ', φ' , and θ'', φ'' do so.

Suppose that $\varphi'_k < \varphi_k$. This implies that $f^{-1}(P)$ around k belongs to class 1, 5, or 6 (Fig. 4). In classes 1 and 5, $\varphi_k = \Delta T_k/P_k$, so that this means $\Delta T'_k < \Delta T_k$, contradicting Eq. (8). In class 6, k makes a negative phase jump due to the firing of $k-1$. $\Delta T'_k = \Delta T_k$ then means $\varphi'_k > \varphi_k$, and $\Delta T'_k \geq \Delta T_k$ implies $\varphi'_k \geq \varphi_k$. Suppose now that $\theta'_{k-1} > \theta_{k-1}$. We have $0 \geq \theta'_{k-1}$. Also, $I \geq P_{\min}$ from Eq. (8). To make the interval I of k as large as the interval P_{\min} of state $f^{-1}(P')$, the larger positive phase jump $0 \geq \theta'_{k-1} > \theta_{k-1}$ must be compensated by a larger negative one, i.e., $0 \leq \varphi'_k < \varphi_k$. But we have already shown that $\varphi'_k \geq \varphi_k$. Thus $\theta'_{k-1} \leq \theta_{k-1}$. That $\varphi_k \geq \varphi''_k$ and $\theta_{k-1} \leq \theta''_{k-1}$ can be shown analogously, or seen by symmetry, since a state of class 4 [as $f^{-1}(P'')$] can be seen as a state of class 1 [like $f^{-1}(P')$] turned upside down, with $\Delta T \rightarrow -\Delta \hat{T}$, $\theta \rightarrow \hat{\varphi}$, and $\varphi \rightarrow \hat{\theta}$, where the hat means that the ordering of the elements has been reversed.

The second part of Eq. (4) can be reexpressed $\theta_k < 0 \Leftrightarrow \varphi_k > 0$. This condition is assumed to be fulfilled by the state $f^{-1}(P')$. When the period of oscillator 1 is continuously increased from P'_1 to P_1 , the k th elements of the phase vectors change continuously from θ'_k, φ'_k to θ_k, φ_k (Fig. 6). The argument above together with $\partial I/\partial P_1 > 0$ (Lemma 2) shows that all intermediate solutions fulfill the first part of Eq. (4). Thus none of these phases can wander through the hatched region. Thus, if θ_k, φ_k is to violate the second half of Eq. (4), one of them must cross the line $\phi = 0$. But if one of them crosses this line, the other must do so simultaneously, since if one of them is zero, then $\Delta T_k = 0$, and then the other phase is also zero. Therefore the second half of Eq. (4) cannot be violated. ■

We have assumed that $a > 0$ (Lemma 2) and regard $a = 0$ as a limiting case. It can also be treated separately and quite simply. One immediately arranges the desired entrained state in a v shape around the fastest oscillator f , which fires

first [as in the state $f^{-1}(P)$ in Fig. 5]. Inserting new oscillators does not perturb the state already created since $a=0$. We have an effective one-way interaction in the directions away from f . $I=P_f$ since f is neither delayed nor advanced.

Proposition 2. Let P_k be a random number from a distribution with support $[P_{\min}, P_{\max}]$. In the limit $N \rightarrow \infty$, the following holds:

(1) If a realization P of the system has an entrained state fulfilling Eq. (4), the probability is one that $I=P_{\min}$.

(2) The probability is zero that the realization has such an entrained state if $g < g_c$.

Proof of Proposition 2. Consider an entrained state with a long sequence of oscillators $m, m-1, m-2, \dots$, with $P_m, P_{m-1}, \dots, < I$. All these have to be delayed. To accomplish the delay of oscillator m it is favorable that $\Delta T_m > 0$. Assume that this is the case. Then, since $a \leq (1-g)^{-1}$, it follows from Eq. (5') that $\Delta T_{m-1} < \Delta T_m$. At some $j > 0$ we must then have $\Delta T_{m-j} < 0$, since if the sequence $\Delta T_m, \Delta T_{m-1}, \dots$ was to converge to zero, oscillators far away in the sequence would not be delayed, contrary to what was required. ΔT_{m-j-1} is then determined by Eq. (5) in case 4 (Fig. 4), giving $\Delta T_{m-j-1} = g^{-1}(P_{m-j} - I) + (1-g)^{-1}\Delta T_{m-j}$. Thus, beyond oscillator $m-j$, the ΔT_k 's drop faster and faster until Eq. (4) is violated. As $N \rightarrow \infty$, the probability of having a long sequence as described above is one for any assumed $I > P_{\min}$, i.e., the probability is one that $I = P_{\min}$. Thus the critical situation may occur that a long sequence of oscillators with period P_{\max} is to be entrained to P_{\min} . This was the situation leading to Eq. (6). Again, as $N \rightarrow \infty$, the probability that such a long sequence is found somewhere in the chain is one. Therefore, in this limit, the probability is zero to have an entrained state of the desired type when $g < g_c$. ■

A finite chain always entrains at some $g < g_c$ if $a > 0$. If $a = 0$, the chain may or may not entrain at a $g < g_c$. It entrains at g_c if and only if the fastest oscillator f has period P_{\min} , and the slowest has period P_{\max} . This is because $I = P_f = P_{\min}$ so that the situation leading to Eq. (6) may occur. When $a = 0$, it occurs already if *one* oscillator has period P_{\max} (see proof of Lemma 1). If $a > 0$, the situation occurs only if a *long sequence* of the chain has period P_{\max} . Loosely speaking, a finite chain more easily entrains at a $g < g_c$ if $a > 0$ than if $a = 0$. This observation was used to interpret the simulation results (Sec. V).

Proposition 3. The entrained states which fulfill Eq. (4) are stable.

Proof of Proposition 3. We investigate the fate of an orbit $\tilde{\phi}(t) = \phi(t) + \delta\phi(t)$, where $\phi(t)$ is a point on the limit cycle corresponding to the entrained state. $\delta\phi$ changes only when one oscillator fires. When k fires, the only components that change are $\delta\phi_{k-1}$ and $\delta\phi_{k+1}$. Say that $\delta\phi \rightarrow \delta\phi'$ when k fires. Looking at Fig. 7,

$$\delta\phi'_{k+1} = \delta\phi_{k+1} + gh(\chi) - gh(\theta_k).$$

We see that

$$\chi = \theta_k + \delta\phi_{k+1} - P_k \delta\phi_k / P_{k+1}.$$

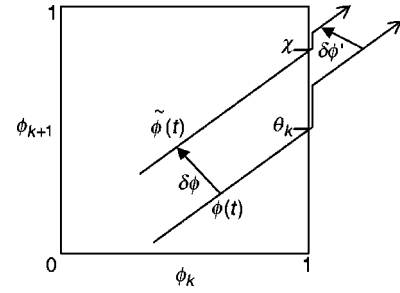


FIG. 7. Projection onto the (ϕ_k, ϕ_{k+1}) -plane of the limit cycle orbit $\phi(t)$ and a perturbed orbit $\tilde{\phi}(t) = \phi(t) + \delta\phi(t)$. When k fires, $\delta\phi_{k+1}$ changes, whereas $\delta\phi_k$ stays fixed.

Thus, if $|\delta\phi|$ is small enough

$$\delta\phi'_{k+1} = \delta\phi_{k+1} + gh'(\theta_k)(\delta\phi_{k+1} - P_k \delta\phi_k / P_{k+1}).$$

An analogous consideration gives $\delta\phi'_{k-1}$. Introducing the vector $\delta\tau$, with components $\delta\tau_k = P_k \delta\phi_k$

$$\begin{cases} \delta\tau'_{k-1} = [1 + gh'(\varphi_{k-1})]\delta\tau_{k-1} - gh'(\varphi_{k-1})\delta\tau_k \\ \delta\tau'_{k+1} = -gh'(\theta_k)\delta\tau_k + [1 + gh'(\theta_k)]\delta\tau_{k+1} \\ \tau'_j = \delta\tau_j, \quad j \neq k-1, k+1 \end{cases} \quad (10)$$

In matrix notation, $\delta\tau' = M_k \delta\tau$. Say that k_1 is the first oscillator that fires after time t_0 , k_2 the second, and so on. Then we have the return map $\delta\tau(t_0 + I) = A \delta\tau(t_0)$, with $A = M_{k_N} \dots M_{k_2} M_{k_1}$. Each matrix M_k , $1 \leq k \leq N$, occurs exactly once in the product. $(1, 1, \dots, 1)$ is an eigenvector of each M_k and has eigenvalue 1. Therefore, it is also an eigenvector of A with eigenvalue 1. It corresponds to a perturbation along the limit cycle. The cycle is stable if all other eigenvalues have moduli < 1 . To show this, we use a corollary to the Perron–Frobenius theorem [25] which states that a positive [26] square matrix B has exactly one positive eigenvector with a positive eigenvalue λ_1 . All other eigenvalues have moduli less than λ_1 . For all natural numbers m , $(1, 1, \dots, 1)$ is an eigenvector to A^m with eigenvalue 1. Therefore it suffices to show that A^m is positive for some m .

It follows from Eq. (4) that M_k is non-negative [26], since $h'(\varphi_k)$ and $h'(\theta_k)$ equal -1 or $-a$, and $0 \leq a, g \leq 1$. Therefore A is also non-negative. Suppose that $\delta\tau$ is non-negative. Let S be the set of oscillators j with $\delta\tau_j > 0$. Choose $S = \{k\}$. It can be seen in Eq. (10) that S changes from $\{k\}$ only when k fires, after which it becomes $\{k-1, k, k+1\}$. S grows one step in the direction of decreasing (increasing) index when the member oscillator with lowest (highest) index fires. It can also be seen in Eq. (10) that S never loses members. Thus $S = \{1, \dots, N\}$ after sufficiently long time. In other words, column k of A^m is positive for some m . Since k is arbitrary, this means that A^m is positive for some m . ■

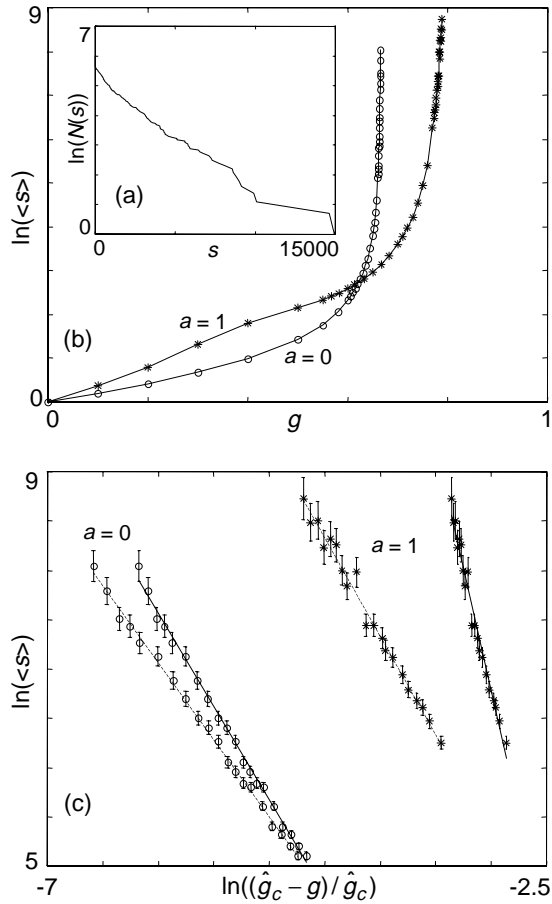


FIG. 8. Properties of the cluster size distribution. Rings correspond to $a=0$, and stars to $a=1$. (a) Cluster sizes were exponentially distributed. $N(s)$ is the number of clusters larger than or equal to s . The parameters $a=1$ and $g=0.78$ were used. (b) Mean cluster sizes $\langle s \rangle$ as functions of g . (c) Test of Eq. (11). The term \tilde{g}_c is defined to be the \hat{g}_c which gives the best fit. For $a=0$, $\hat{g}_c = g_c = 2/3$ gave $\alpha = 1.89$ (solid line), while $\tilde{g}_c = 0.6662$ gave $\alpha = 1.56$ (dashed line). For $a=1$, $\hat{g}_c = g_c = \sqrt{2/3}$ gave $\alpha = 5.05$ (solid line), while $\tilde{g}_c = 0.7953$ gave $\alpha = 1.99$. Error bars are approximate 95% confidence intervals (see Ref. [28]).

IV. SIMULATIONS

The behavior of the system around g_c was studied by means of simulation. The natural periods were taken from a square distribution with $1 \leq P_k \leq 1.5$ [17]. The PRC is specified in Fig. 1. A chain of 500 000 oscillators was used.

We note first that for $g > g_c$, the chain always seemed to approach an entrained state which fulfills Eq. (4).

Figure 8(a) shows a cluster size distribution for $g=0.78$ and $a=1$. In this case $g_c = \sqrt{2/3} \approx 0.816$ [Eq. (7)]. The distribution is exponential to a good approximation [27]. This seemed to be the case for all $g < g_c$ and all a . No tendency towards a critical, power law distribution at g_c was seen. Figure 8(b) shows that the mean cluster sizes $\langle s \rangle$ diverge as $g \rightarrow g_c$. In Fig. 8(c), the divergences are fitted to power laws

$$\langle s \rangle \propto (\hat{g}_c - g)^{-\alpha}. \quad (11)$$

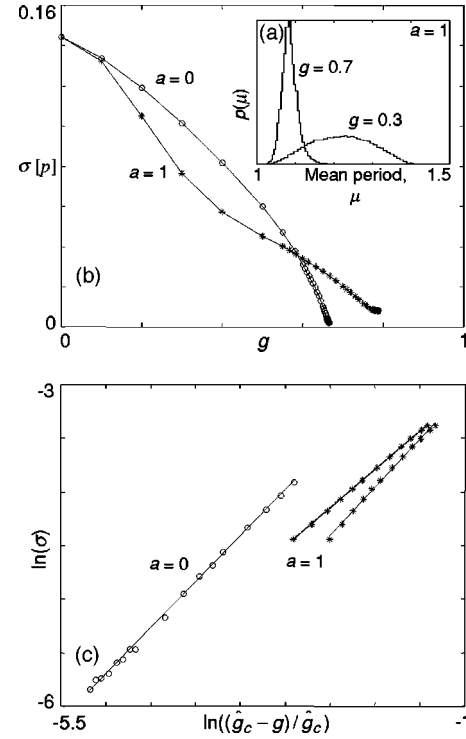


FIG. 9. Properties of the mean period distribution. Rings correspond to $a=0$, and stars to $a=1$. (a) Mean period distribution p for $g=0.3$ and $g=0.7$ for $a=1$. (b) Standard deviation $\sigma[p]$. (c) Test of Eq. (12). For $a=0$, $\hat{g}_c = g_c$ gave $\beta = 0.86$, whereas $\hat{g}_c = \tilde{g}_c = 0.6669$ gave $\beta = 0.88$ (not shown). For $a=1$, $\hat{g}_c = g_c$ gave $\beta = 0.89$ (solid line), while $\hat{g}_c = \tilde{g}_c = 0.7920$ gave $\beta = 0.71$.

The term \tilde{g}_c is defined to be the \hat{g}_c that gives the best fit. For both values of a , $\tilde{g}_c < g_c$. In the case $a=0$, both g_c and \tilde{g}_c gave rise to acceptable fits, given the confidence intervals [28]. For $a=1$, the fit for $\hat{g}_c = g_c$ was barely acceptable. If $\hat{g}_c = g_c$ was used for both values of a , it would be clear that $\alpha_{a=0} \neq \alpha_{a=1}$, so that α becomes a system dependent critical exponent. However, the estimated α is very sensitive to the choice of \hat{g}_c , and it is not at all clear that $\hat{g}_c = g_c$ is appropriate in the simulations. To test the numerical stability of \tilde{g}_c in the case $a=1$, first $T_r = 5000$ and $T_m = 2000$ was used for $\delta P = 0.002$ (Sec. II), then δP in the range $[0.0005, 0.003]$ was used for the standard $T_r = T_m = 1000$. This caused \tilde{g}_c to vary in the interval $[0.7943, 0.7964]$, giving α in the interval $[1.714, 2.113]$. The choice of these parameters thus does not seem to be responsible for the underestimation of g_c . It is, therefore, possible that the system used in the simulations indeed tends to entrain at a g significantly lower than g_c , and thus one cannot exclude the possibility that $\alpha_{a=0} = \alpha_{a=1}$. Probably, a reliable answer to the question of universality can only be found by analytical argument.

Figure 9(a) shows the mean period distribution in the chain for two different values of g for $a=1$. The standard deviation σ decreases when g increases. σ measures the amount of disorder in the system, and is quite analogous to the entropy. Figure 9(b) shows σ as a function of g . The finite simulation time gave rise to a residual σ because of

remaining transients and a finite measurement time. In the figure, this can be seen as a flattening of the $a=1$ curve close to g_c . In Fig. 9(c) the convergences of σ to zero are fitted to power laws

$$\sigma \propto (\hat{g}_c - g)^\beta. \quad (12)$$

The data seem consistent with this assumption, even if no error bars are estimated for σ . Because of the residual σ , I did not go any closer to g_c than the point where σ from simulations with $T_t=5000$ and $T_m=2000$ started to drop below σ from the standard simulations with $T_t=T_m=1000$. For $a=1$, \tilde{g}_c was again significantly lower than g_c . For the same reasons as for α , the question whether β is universal or not must be left open.

V. DISCUSSION

The fact that the estimated critical coupling \tilde{g}_c extrapolated from the data is smaller than the analytical g_c , and that the difference is greater in the case $a=1$, is consistent with the remark made after Proposition 2. There it was stated that a finite chain tends to entrain below g_c , and that this tendency is more pronounced when $a>0$. This suggests that the error in the estimation is primarily a finite size effect, and not due to numerical errors. Thus a value of \hat{g}_c lower than g_c should be inserted in Eqs. (11) and (12). Therefore, the possibility should not be discarded that the critical exponents for the system with $a=0$ are equal to those for the systems with $a=1$.

The possibilities have not been considered that for $g > g_c$, other attractors may coexist with the entrained state fulfilling Eq. (4), or that other stable entrained states may exist for $g < g_c$. This would make the phase transition less well defined. However, no indications of this were seen. All simulations were consistent with the hypothesis that the only entrained states that existed were those fulfilling Eq. (4). Nevertheless, in the case of a two-oscillator system, it was shown by Ikeda [10] that such entrained states could coexist either with entrained states where the oscillators triggered each other, or with states where they delayed each other. Generally, mutual triggering requires a small ϕ_+ , whereas mutual delay requires a large ϕ_- .

That σ drops continuously to zero at g_c , apparently according to a power law, indicates that we have an analogue to a continuous (critical) phase transition. The power law divergence of $\langle s \rangle$ is similar to the divergence of the correlation length at the critical point. However, the cluster size distribution is not critical at g_c . Preliminary simulations indicate that in two dimensions, there is an even closer analogue to a critical phase transition. There, the size s_{\max} of the largest cluster diverges at a critical coupling, after which the smaller clusters become islands in an entrained sea, just like islands of opposing spins in an Ising magnet below T_c . At the critical coupling, the cluster sizes are critically distributed. As g increases further, the islands get smaller, and finally the whole lattice frequency entrains at a second critical coupling. The order parameter

$$r \equiv \lim_{N \rightarrow \infty} s_{\max}/N$$

seems to increase continuously from zero at the first phase transition, and saturate at one at the second. A fuller account of these simulations will be presented within a short time. Note that in one dimension, r jumps discontinuously from zero to one at g_c , since cluster sizes $\mathcal{O}(N)$ cannot coexist with an island density larger than zero. In this sense, the phase transition described in this paper is first order. This might have something to do with the absence of a critical cluster size distribution at g_c .

Two-dimensional lattices of locally coupled, pulse-coupled oscillators with random natural frequencies have been studied numerically by Corral, Pérez, and Díaz-Guilera [29]. They used the Peskin type of interaction (Sec. I), and studied avalanches, i.e., regions that fire at the same time due to infinitely fast firing transmission. Their simulations suggested that the size distribution of the avalanches was critical for a range of parameter values, indicating self-organized criticality (SOC). No signs of SOC have been seen in the present simulations; in the one-dimensional chain, the cluster size distribution was *never* critical (Sec. IV), and in the two-dimensional case the critical point seemed well defined. The different results might be due to the fact that avalanches are not directly related to frequency clusters. The sizes and locations of avalanches may vary from time to time, whereas frequency clusters by definition are time-independent regions. However, if a system displays SOC as judged from the avalanche size distribution, it should do so as judged from the cluster size distribution (assuming that stationary clusters do exist). Therefore, it is more plausible that the differing behaviors are due to qualitative differences between our systems. For example, avalanches are not allowed in the system studied here, unless the coupling is infinite ($g=1$).

The assumption of a finite frequency bandwidth may seem unnatural. In the case of cardiac pacemaker cells, there is a lower bound on the natural period set by the refractory period, during which the cell is recovering and no new action potential can be initiated. However, there is no apparent upper bound. The excitable, impulse-transmitting nonpacemaker cells may be seen as oscillators with infinite natural period. Like all other excitable cardiac cells, these can be triggered shortly after a preceding firing, so that the entire heart can entrain to a common frequency. The problem with our model is that the PRC is independent of the natural period P_k . This means that during a time $\phi_- P_k$ oscillator k can only be delayed, so that it cannot be entrained to a period shorter than this. Therefore, our model can simulate cardiac tissue realistically only if a quite narrow bandwidth is assumed. The occurrence of long natural periods would make impossible any phase transition to states with order parameter $r>0$ in a one-dimensional chain, since such slow oscillators would break the entrainment at finite intervals. In multidimensional lattices, however, the slow oscillators could be islands in an entrained sea, so that states with $r>0$ were possible, but states with $r=1$ still impossible.

To get a deeper understanding of the kind of phase transitions described in this paper, one should ideally invent a renormalization group from which critical exponents can be deduced, and their possible universality determined. In this

way, a proper classification of the phase transitions might also be obtained. As discussed above, the transition in the one-dimensional chain had features reminiscent both of a first- and second-order transition.

-
- [1] A. T. Winfree, *J. Theor. Biol.* **16**, 15 (1967).
- [2] A. T. Winfree, *The Geometry of Biological Time* (Springer, New York, 1980).
- [3] Y. Kuramoto, *Prog. Theor. Phys. Suppl.* **79**, 223 (1984).
- [4] Frequency clusters have been found experimentally in the rhythmic electric activity of the small intestine. In the intact organ, the frequency decreased in steps in the direction away from the stomach. In contrast, the frequencies of small pieces cut from the intestine decreased continuously [N. E. Diamant and A. Borthoff, *Am. J. Physiol.* **216**, 301 (1969)].
- [5] H. Sakaguchi, S. Shinomoto, and Y. Kuramoto, *Prog. Theor. Phys.* **77**, 1005 (1987).
- [6] S. H. Strogatz and R. E. Mirollo, *Physica D* **31**, 143 (1988).
- [7] H. Sakaguchi, S. Shinomoto, and Y. Kuramoto, *Prog. Theor. Phys.* **79**, 1069 (1988).
- [8] N. Kopell and G. B. Ermentrout, *Commun. Pure Appl. Math.* **39**, 623 (1986).
- [9] J. L. Rogers and L. T. Wille, *Phys. Rev. E* **54**, R2193 (1996).
- [10] N. Ikeda, *Biol. Cybern.* **43**, 157 (1982).
- [11] A. A. Brailove, *Int. J. Bifurcation Chaos Appl. Sci. Eng.* **2**, 341 (1992).
- [12] R. E. Mirollo and S. H. Strogatz, *SIAM J. Appl. Math.* **50**, 1645 (1990).
- [13] A. Díaz-Guilera, C. J. Pérez, and A. Arenas, *Phys. Rev. E* **57**, 3820 (1998); A. Díaz-Guilera and C. J. Pérez-Vicente, *Int. J. Bifurcation Chaos Appl. Sci. Eng.* **9**, 2203 (1999).
- [14] W. Senn and R. Urbanczik, *SIAM (Soc. Ind. Appl. Math.) J. Appl. Math.* **61**, 1143 (2001).
- [15] T. Sano, T. Sawanobori, and H. Adaniya, *Am. J. Physiol.* **235**, H379 (1978); J. Jalife *et al.*, *ibid.* **238**, H307 (1980); J. M. B. Anumonwo *et al.*, *Circ. Res.* **68**, 1138 (1991).
- [16] The size of the rabbit sinus node is roughly $2 \times 5 \times 0.2$ mm. (Fig. 4 in [I. Ten Velde *et al.*, *Circ. Res.* **76**, 802 (1995)]). A typical rabbit sinus node cell volume is $5000 \mu\text{m}^3$ [J. C. Denyer and H. F. Brown, *J. Physiol. (London)* **428**, 405 (1990)]. This gives $\approx 400\,000$ cells.
- [17] The firing interval ratio between the fastest and slowest rabbit sinus node cells is at least two [H. Honjo and M. R. Boyett, *J. Physiol. (London)* **452**, 128P (1992)]. Each cell also shows a firing interval variability of up to 10% [T. Opthof *et al.*, *J. Mol. Cell. Cardiol.* **19**, 923 (1987)].
- [18] M. Masson-Pévet, W. K. Bleeker, and D. Gros, *Circ. Res.* **45**, 621 (1979); W. K. Bleeker *et al.*, *ibid.* **46**, 11 (1980).
- [19] P. Östborn, B. Wohlfart, and G. Ohlén, *J. Theor. Biol.* **211**, 201 (2001); P. Östborn, G. Ohlén, and B. Wohlfart, *ibid.* **211**, 219 (2001).
- [20] C. S. Peskin, *Mathematical Aspects of Heart Physiology* (Courant Institute of Mathematical Sciences, New York University, New York, 1975).
- [21] W. K. Bleeker *et al.*, *Circ. Res.* **46**, 11 (1980).
- [22] J. Buck, *Q. Rev. Biol.* **63**, 265 (1988).
- [23] A. H. Cohen, P. J. Holmes, and R. H. Rand, *J. Math. Biol.* **13**, 345 (1982).
- [24] This is the main difference to system (1). There, if $\Delta T_{k-1} = \Delta T_k$ in an entrained state, k fires with its natural period since the sine function is odd. Thus, the $|\Delta T_k|$'s grow without bound if a longer and longer section of the chain is to be advanced (or delayed). In the system used here, this problem arises only in the delay case (see proof of Proposition 2).
- [25] P. Lancaster, *Theory of Matrices* (Academic, New York, 1969).
- [26] A vector or matrix is positive (non-negative) if all elements are positive (non-negative) real numbers.
- [27] The two largest clusters are somewhat oversized. Close to g_c there was typically one or two such clusters. I tentatively attribute this to the finite δP (Sec. II). As g_c is approached from below, the frequency difference between two neighbor clusters decreases (Fig. 9), so that it at some point is typically less than δP . After that, the cluster sizes are severely overestimated. Specifically, it is the large clusters that have similar frequencies, while the smaller ones are more extreme (not shown).
- [28] Ninety five percent confidence intervals were calculated from the assumption of exponential cluster size distribution. This led to the result that if the number of clusters is large, $\ln\langle s \rangle$ is normally distributed with variance $\langle s \rangle / N$. The intervals are therefore $\ln\langle s \rangle \pm 1.96 \sqrt{\langle s \rangle / N}$.
- [29] A. Corral, C. J. Pérez, and A. Díaz-Guilera, *Phys. Rev. Lett.* **78**, 1492 (1997).
- [30] N. Kopell and G. B. Ermentrout, *SIAM J. Appl. Math.* **50**, 1014 (1990).